Unexpected Photophysical Properties of Symmetric Indolylmaleimide Derivatives[†]

Başak Kükrer Kaletaş,[‡] Christian Mandl,[§] Gert van der Zwan,[‖] Marianna Fanti,[⊥] Francesco Zerbetto,[⊥] Luisa De Cola,[‡] Burkhard König,*,[§] and René M. Williams*,[‡]

Molecular Photonic Materials, van't Hoff Institute for Molecular Sciences, Universiteit van Amsterdam, Nieuwe Achtergracht 166, 1018 WS Amsterdam, The Netherlands, Institut für Organische Chemie, Universität Regensburg, D-93040 Regensburg, Germany, Vrije Universiteit, De Boelelaan 1083, 1081 HV Amsterdam, The Netherlands, and Dipartimento di Chimica "G. Ciamician", University of Bologna, via Selmi 2, I-40126 Bologna, Italy

Received: March 1, 2005; In Final Form: May 22, 2005

Arcyriarubin A and arcyriaflavin A, two strongly emissive and intensely colored natural products containing both two indoles and a maleimide unit, are investigated (in the flavin the two indole moieties are coupled by a cyclization). The photophysical properties of these compounds were studied in several solvents using UV–vis absorption, steady-state and time-resolved emission, nano- and femtosecond transient absorption spectroscopy. Furthermore, the effect of complexation with zinc(II) 1,4,7,11-tetraazacyclododecane on the photophysical properties of these natural products has been investigated. The chemical structures of the compounds would suggest a charge transfer (CT) character in the ground and/or excited states, since indole is a well-known electron donor and maleimide is a good electron acceptor. Their solvatochromic behavior was investigated by using the Kamlet–Taft approach and indicates only a small CT character in the excited state. This is substantiated by the time-resolved spectroscopy and the complexation study. Molecular orbital calculations indicate that there are no electronic transitions in which a large electron density is transferred from one indole unit to the maleimide part. All calculated orbitals show a strong delocalization of the electron density over the whole molecule. These findings corroborate the experimental results. Whereas the two compounds do have a substantial (calculated) ground-state dipole moment (6 D) and show some solvatochromic behavior, they behave more like conjugated aromatic systems than like electron donor–acceptor systems.

Introduction

The research conducted on bisindolylmaleimide derivatives has two goals: pharmaceutical applications as new drugs[1–9] and photonic applications, for instance as components in red-emitting light emitting diodes (LEDs).[10] The majority of the research is conducted in the pharmaceutical area and is aimed at efficient and versatile methods to synthesize indolylmaleimide derivatives. Some of these derivatives are selective inhibitors of protein kinase C (PKC). This isoenzyme family is believed to play an essential role in many signal transduction pathways[1] and is implicated in a wide range of physiological processes. Several macrocyclic bisindolylmaleimide derivatives show promising results as novel therapy agents for autoimmune diseases, especially diabetes and cancer.[2] The double bond of the maleimide ring and the presence of hydrogen-bond donor ability in the maleimide unit appear to be essential in the activity of these agents.[3] The bisindolylmaleimide subunit is present in a number of biologically active metabolites isolated from Streptomycetes, including staurosporine[4] and rebeccamycin.[5] The simplest members of this class of compounds are the arcyriarubins, a family of pigments that were isolated from the fruiting bodies of the slime mold, *Arcyria denudata*, more than 20 years

ago by Steglich et al.[5] Since arcyriarubin A (*N*–H bisindolylmaleimide, here abbreviated as **BIM**) is the core structure for these derivatives, several research groups are developing efficient and versatile synthetic methods for this class of compounds. Consequently, many derivatives of the parent bisindolylmaleimide structure have been synthesized and tested to explore as a lead structure.[6–8] Arcyriaflavin (cyclized *N*–H bisindolylmaleimide, here abbreviated as **C-BIM**) analogues are currently being evaluated in human clinical trials as anticancer drugs.[9] In the area of photonic applications, the use of bisindolylmaleimide derivatives as an effective red electroluminescent material has been demonstrated. Most bisindolylmaleimide compounds are intensively red solids, and some show strong red luminescence in solution. Recently, Chow et al. used a number of *N*-methylated bisindolylmaleimide derivatives in the fabrication of LEDs.[10] The formation of amorphous films with red emission in the solid state, good thermal stability, and reversible oxidation are essential characteristics for this application. Including this recent work, still very little is known about the spectroscopic properties of bisindolylmaleimides. The origin of their intense color as a solid and their strongly emissive properties in solution have not been fully understood. To our knowledge, detailed investigations of the photophysical properties of such compounds have not been reported until now.

Here we discuss the spectroscopic properties of two symmetric bisindolylmaleimide derivatives, **BIM** and **C-BIM** (Scheme 1). The *N,N*-alkyl-functionalized bisindolylmaleimide (**N-BIM**) is used as a model compound with improved solubility and the inability to act as a hydrogen-bond donor. As reported


[†] We dedicate this paper to Prof. W. Steglich.
* To whom correspondence should be addressed. E-mails: (R.M.W.) williams@science.uva.nl; (B.K.) burkhard.koenig@chemie.uni-regensburg.de.
[‡] Universiteit van Amsterdam.
[§] Universität Regensburg.
[‖] Vrije Universiteit.
[⊥] University of Bologna.

Symmetric Indolylmaleimide Derivatives

J. Phys. Chem. A, Vol. 109, No. 29, 2005 **6441**

SCHEME 1: Compounds under Investigation (BIM, C-BIM, and N-BIM) and Their Complex Formation with Zn(II)-cyclen
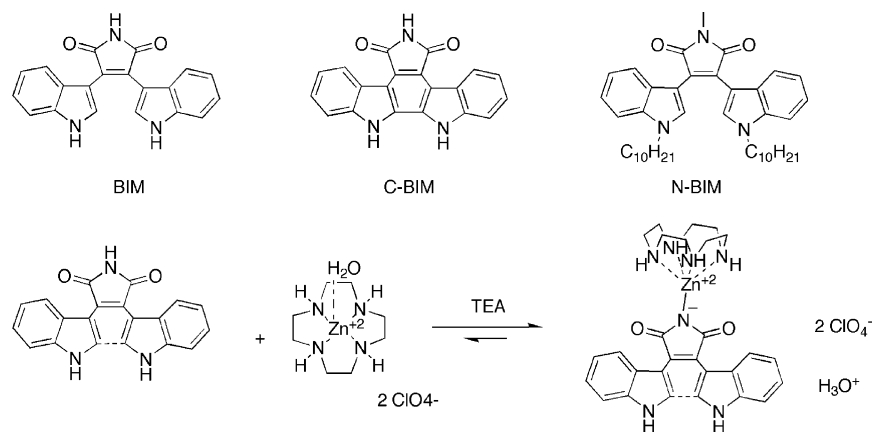
SCHEME 2: Synthesis of BIM and C-BIM Chromophores
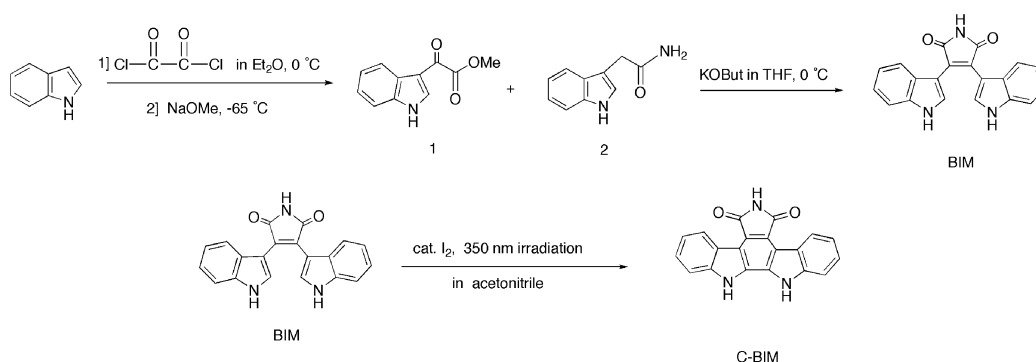
elsewhere[11,12] for the asymmetric monoindolylmaleimides, the complexation of **BIM** and **C-BIM** with zinc(II) 1,4,7,11-tetraazacyclododecane (named as Zn(II)−cyclen; Scheme 1) via noncovalent interaction was studied, as well.

UV−vis absorption, steady-state and time-resolved emission, nano- and femtosecond transient absorption in combination with the results of computational studies were used to explain the light-induced processes in these compounds.

Results and Discussion

Synthesis of the BIM, C-BIM, and N-BIM. Since **BIM** is the core structure for many derivatives, several research groups are working on its efficient synthesis. The most widely used method to produce **BIM** involves the reaction of indolylmagnesium bromide with a 2,3-dihalomaleimide.[13] A more efficient way to synthesize 2,3-bis(1*H*-indol-3-yl)maleimide (**BIM**) was developed recently by Faul et al.[14] and is used in this study as well. The method involves reaction of methyl indole-3-glyoxylate with commercially available indole-3-acetamide using a 1.0 M solution of KOBu^t in tetrahydrofuran (THF; Scheme 2).

12,13-Dihydro-5*H*-indolo[2,3-*a*]pyrrolo[3,4-*c*]carbazole-5,7-(6*H*)-dione (**C-BIM**)[9] is synthesized by overnight irradiation at 350 nm of a solution of **BIM** in a photochemical reactor, in the presence of I$_2$ as oxidizing agent in acetonitrile (Scheme 2). The reference compound, **N-BIM**, was prepared according to literature procedures. The detailed synthetic procedures, including purification and characterization, are given in the Experimental Section.

Steady-State Spectroscopy. The symmetric indolylmaleimides **BIM, C-BIM**, and **N-BIM** consist of two parts: the well-known electron acceptor, maleimide, and the electron donor, indole. In general, charge separation can be expected in the
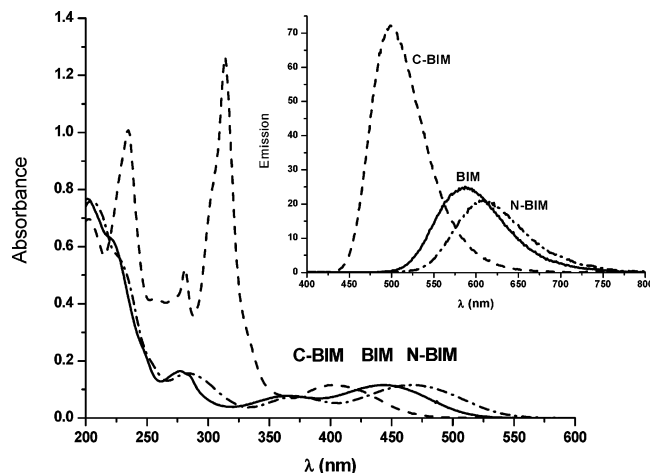

Figure 1. UV−vis absorption spectra of compounds **BIM** (solid line), **C-BIM** (dashed line), and **N−-BIM** (dashed−dotted line) in acetonitrile. Emission spectra (inset) of **BIM** (solid line), **C-BIM** (dashed line), and **N-BIM** (dashed−dotted line) in aerated acetonitrile solution (λ_{ex} = 370 nm; A_{370} = 0.1).

ground and/or excited state for strong electron donor−acceptor systems. However, for these systems the results are not as trivial as expected, and in the case of the indolylmaleimide compounds, the experiments showed unexpected photophysical properties.

In Figure 1, room-temperature UV−vis absorption and emission spectra (inset) of the compounds **BIM, C-BIM**, and **N-BIM** in acetonitrile solution are presented. The separate components, indole and maleimide, do not show absorption at energy lower than 300 and 325 nm, respectively. Clearly, the covalent functionalization of maleimide with two indole groups induces mixing of the electronic states, creating other low-lying

TABLE 1: Absorption Maxima, Emission Maxima, and Emission Quantum Yields (Φ) of the Compounds under Investigation[a]

	BIM			C-BIM			N-BIM	
solvents	λ_{abs} (nm) (ϵ)	λ_{em} (nm)	Φ	λ_{abs} (nm) (ϵ)	λ_{em} (nm)	Φ	λ_{abs} (nm)	λ_{em} (nm)
Chex	b	b	b	b	b	b	462	556
TOL	447	552	0.28	398	465		472	580
DBE	445	550	0.22	393	461	0.28	469	570
DIE	443	544	0.28	391	450	0.25	470	570
EA	445	560	0.21	398	473	0.29	472	585
THF	450	567	0.24	400 (5522)	475	0.44	471	586
DCM	448 (7080)	582	0.21	401	492	0.18	477	613
DMF	454 (7290)	584	0.13	409	503	0.25	474	612
EtOH	460 (7004)	640	0.003	405 (5137)	550	0.26	480	646
ACN	446 (6850)	585	0.10	402 (5588)	500	0.33	470	610

[a] ϵ is the molar extinction coefficient in M^{-1} cm^{-1}. Data are in increasing order of polarity of solvents. Chex, cyclohexane; TOL, toluene; DBE, dibutyl ether; DIE, diisopropyl ether; EA, ethyl acetate; THF, tetrahydrofuran; DCM, dichloromethane; DMF, *N,N*-dimethylformamide; EtOH, ethanol; ACN, acetonitrile. [b] Not soluble.

excited states. This gives rise to low-energy absorption bands and results in colored compounds.

In e.g. acetonitrile, **BIM** and **N-BIM** show two major absorption bands, one in the visible region around 446−470 nm, with shoulders at 366−370 nm, and one around 277−285 nm in the UV region, which can be assigned to $\pi-\pi^*$ transitions from the S_0 to the S_1 and S_2 states, respectively. Changing the N-substituent from hydrogen to methyl does not result in a significant difference in the UV−vis spectrum; neither does the *N*-alkylation of the indole moieties (see **N-BIM**). The visible absorption band gives the compounds their distinct red color in their solid form as well as additional new spectroscopic properties.

In contrast, **C-BIM** shows a completely different absorption spectrum as compared to **BIM** and **N-BIM**. Besides the $\pi-\pi^*$ band at 402 nm, sharp intense peaks were observed at 235, 281, and 314 nm, reminiscent of flat aromatic systems such as dibenz-(*a,h*)anthracene. These intense bands are assigned to the $S_0 \rightarrow S_2$ transitions with higher transition probability than for the open **BIM** compound. Whereas the π-systems within **BIM** and **N-BIM** are not fully conjugated due to the torsion of the indole rings out of the maleimide plane forced by steric interactions, **C-BIM** has indeed a flat structure.

When irradiated at 370 nm, **BIM** and **N-BIM** exhibit intense red luminescence at 585−610 nm (Figure 1, inset). Changing the substituents on the N atom (compare **BIM** to **N-BIM**) does not influence this red emission. On the other hand, **C-BIM** shows emission at 500 nm (with higher intensity), i.e., shifted to higher energy as also observed in the absorption spectrum.

The emission spectra of **BIM**, **N-BIM**, and **C−BIM** (see Figure 1, inset) were recorded upon excitation in the long-wavelength absorption band. In contrast to the asymmetric indolylmaleimide derivatives investigated,[11,12] the emission of these symmetric bisindolylmaleimide systems is rather high (average Φ = 0.25). Absorption and emission maxima (λ), molar extinction coefficients (ϵ), and emission quantum yields (Φ) were obtained in a series of solvents of different polarities and are summarized in Table 1. Emission quantum yields for **N-BIM** were not determined.

The spectral values are reported in order of increasing solvent polarity. As can be seen in Table 1, both **BIM** and **C-BIM** have rather high quantum yields in nonpolar solvents. Only in ethanol, the emission quantum yield of **BIM** is strongly quenched (see later), and also in polar solvents such as dimethylformamide (DMF) and acetonitrile, the quantum yield is only around 10%. On the other hand, the emission quantum yields of the **C-BIM** range from 18 to 44%, including the value in ethanol. The relatively lower quantum yields of **BIM** in polar protic solvents

indicate strong solute−solvent interactions that also affect the energy level of the emitting state.

To explain if other factors besides polarity could play a role in the quenching of the emission, we have investigated the effect of a possible proton transfer in polar protic solvents. The deuterium isotope test[15a] has been performed on **BIM**. For this purpose, the emission spectrum of the compound was recorded in methanol and CD3OD solution, respectively. An enhancement (~3.2-fold) in emission intensity was detected in the case of the deuterated solvent. This result indicates hydrogen-bonding interactions between the carbonyl groups of the imide function and H(D) of the methanol and/or proton exchange of the NH.

Solvatochromism. A $\pi-\pi^*$ state with charge-transfer (CT) character is expected to be the lowest excited state in these symmetric systems. A blue shift of the emission maximum when going from room temperature to 77 K in a butyronitrile matrix (957 cm^{-1} for **BIM** and 455 cm^{-1} for **C-BIM**) and the enhancement in the emission quantum yield when going to less polar solvents for **BIM** (see Table 1) suggests the same result. Surprisingly, the situation is more complicated than expected.

By comparing the absorption and emission maxima in Table 1, it is not obvious whether the systems show solvatochromic behavior. There is a slight bathochromic shift observed for the absorption and emission maxima when going from nonpolar to more polar solvents. However, it is hard to conclude that there is a real trend. The data of **BIM** and **C-BIM** have been analyzed by using the Kamlet−Taft solvent polarity scale. The treatment is based on the use of a multiparameter equation, called *linear solvation energy relationship* (LSER).[15b]

$$XYZ = (XYZ)_0 + s(\pi^* + d\delta) + a\alpha + b\beta + m\delta_H^2$$

where $(XYZ)_0$, s, a, b, and m are solvent-independent coefficients characteristic of the process under study and indicative of its susceptibility to the solvent properties π^*, α, β, and δ_H^2.

The Kamlet−Taft π^* value is known as an index of solvent dipolarity/polarizability, i.e., the ability of a solvent to stabilize a charge and/or dipolar molecule. By using this parameter it is possible to obtain a correlation between the energy maxima of both the absorption and the emission and the properties of solvents. The π^* scale is derived from solvent effects on the $\pi-\pi^*$ absorptions of the seven nitroaromatics used as primary probe molecules.[15−18]

Other solvatochromic parameters, α and β, are also given in Table 2. The α scale describes the hydrogen-bond donor acidity, and the β scale describes the hydrogen bond acceptor basicity of the solvents. The δ_H is the Hildebrand solubility parameter.

Symmetric Indolylmaleimide Derivatives

J. Phys. Chem. A, Vol. 109, No. 29, 2005 **6443**

TABLE 2: Solvent Parameters and Spectroscopic Data of BIM, C-BIM, and N-BIM in Various Solvents at Room Temperature[a]

solvents	Kamlet−Taft params			BIM			C-BIM			N-BIM		
	π^*	a	b	λ_{abs} (nm)	λ_{em} (nm)	Δ (cm^{-1})	λ_{abs} (nm)	λ_{em} (nm)	Δ (cm^{-1})	λ_{abs} (nm)	λ_{em} (nm)	Δ (cm^{-1})
Chex	0.00	0.00	0.00	*b*	*b*	*b*	*b*	*b*	*b*	462	556	3659
DBE	0.24	0.00	0.46	445	550	4290	393	461	3753	469	570	3750
DIE	0.27	0.00	0.49	443	544	4191	391	450	3353	470	570	3733
TOL	0.54	0.00	0.11	447	552	4255	398	465	3620	472	580	3945
EtOH	0.54	0.83	0.77	460	640	6114	405	550	6510	480	646	5353
EA	0.55	0.00	0.45	445	560	4615	398	473	3984	472	585	4092
THF	0.58	0.00	0.55	450	567	4586	400	475	3947	471	586	4167
ACN	0.75	0.19	0.31	441	585	5582	402	499	4836	467	610	5020
DCM	0.82	(0.30)	0.00	448	582	5139	401	492	4612	477	613	4651
DMF	0.88	0.00	0.69	454	584	4903	409	503	4569	474	612	4757

[a] Data are in increasing order of π^*. Δ is the Stokes shift in cm^{-1}. See Table 1 for abbreviations. [b] Not soluble.
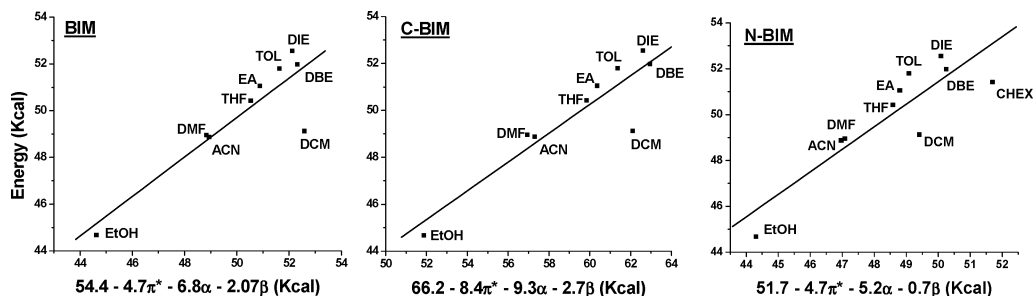
Figure 2. Emission energy maxima of **BIM, C-BIM**, and **N-BIM** plotted vs eqs **1−3**.

It is a measure of the solvent/solvent interactions that are interrupted in creating a cavity for the solute (the cavity term).[19,20]

In Table 2, the absorption and emission maxima and the Stokes shifts for **BIM, C-BIM**, and **N-BIM** are summarized in solvents of different polarity and are sorted according to the increasing order of π^*. As can be seen in Table 2, the absorption maximum undergoes a slight red shift for both compounds when going from dibutyl ether to DMF (from 445 to 454 nm for **BIM,** from 393 to 409 nm for **C-BIM,** and from 462 to 474 nm for **N-BIM**). However, the shifts in emission maxima are larger, thereby leading to an increase in the Stokes shift (Table 2). Both the absorption and the emission maxima in ethanol show the major deviation from the trend for these three compounds. Both the emission maxima and Stokes shifts increase with increasing π^* parameter, which suggests a positive solvatochromic effect.

The linear regression analysis for the relation between the emission maxima of **BIM, C-BIM**, and **N-BIM** and the independent parameters π^*, α, and β gives

$$E_{max}(\text{BIM})/\text{kcal} = (54.4 \pm 0.4) - (4.7 \pm 0.5)\pi^* - (6.8 \pm 0.45)\alpha - (2.07 \pm 0.64)\beta \quad (1)$$

$$E_{max}(\text{C-BIM})/\text{kcal} = (66.2 \pm 0.9) - (8.4 \pm 1.2)\pi^* - (9.3 \pm 1.0)\alpha - (2.7 \pm 1.4)\beta \quad (2)$$

$$E_{max}(\text{N-BIM})/\text{kcal} = (51.7 \pm 0.2) - (4.7 \pm 0.4)\pi^* - (5.2 \pm 0.4)\alpha - (0.7 \pm 0.4)\beta \quad (3)$$

In the case of **N-BIM**, the contribution of β is smaller and has a relatively large error; however, neglecting it does not improve the fit. Clearly the solvent is incapable of acting as a hydrogen-bond acceptor for this system.

When the emission maxima of **BIM, C-BIM**, and **N-BIM** are plotted versus the eqns **1, 2,** and **3** containing the Kamlet−Taft parameters, the plots shown in Figure 2 are obtained by fitting with the multiple regression method.

The negative coefficients for the π^* values in these equations indicate a positive solvatochromism. As the π^* value of the solvent increases, a red shift in the absorption and/or emission maxima is observed. Additionally, both α and β parameters should be taken into account for these symmetric bisindolyl-maleimides. The increased polarizability of the medium and hydrogen-bonding capacity of the solvent lowers the energy of the excited state of the molecules.

According to the Kamlet−Taft treatment, there is a slightly solvatochromic trend in the emission data of all compounds. It is interesting to note that **BIM** and **C-BIM** have relatively high ground-state dipole moments (6.17 D for **BIM** and 6.22 D for **C-BIM**: see computational section).

Complex Formation with Zn(II)−Cyclen. The coordination of the imide group with the Zn(II)−cyclen has been intensively studied,[21−23] and the formation of a bond between the deprotonated imide nitrogen atom and the zinc(II) ion was confirmed by X-ray structures.[24] Strong enhancement effects on the emissive properties of asymmetric indolylmaleimides have been observed and were interpreted as a reduction in acceptor strength due to complexation.[11]

We have followed the assembly of Zn(II)−cyclen via a coordinative bond to **BIM** and **C-BIM** by titration experiments. A stoichiometric amount of Zn(II)−cyclen is added to a solution of **BIM** (2.5×10^{-5} mol L^{-1}) in order to form the adduct **BIM/Zn** (see Scheme 1). In aerated acetonitrile, the complex formation was followed by UV−vis absorption and emission spectroscopy (Figure 3). To favor the deprotonation of the imide to form the zinc−nitrogen bond, a weak base (1 equiv of triethylamine, TEA) was added. Upon addition of Zn(II)−cyclen a blue shift (733 cm^{-1}) of the absorption band centered at 444 nm was observed. Furthermore, a decrease in the molar extinction coefficient of this band and a broadening of the UV band of 280 nm occurs during the assembly process (Figure 3).

The change in emission properties of the **BIM** upon complex formation is rather surprising, since only a small blue shift (387 cm^{-1}) and no change in emission intensity was observed. The
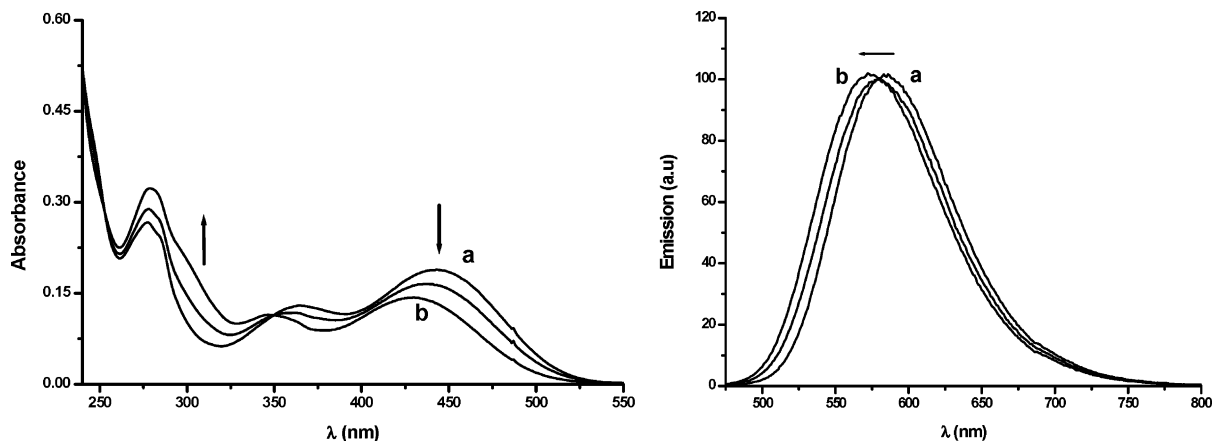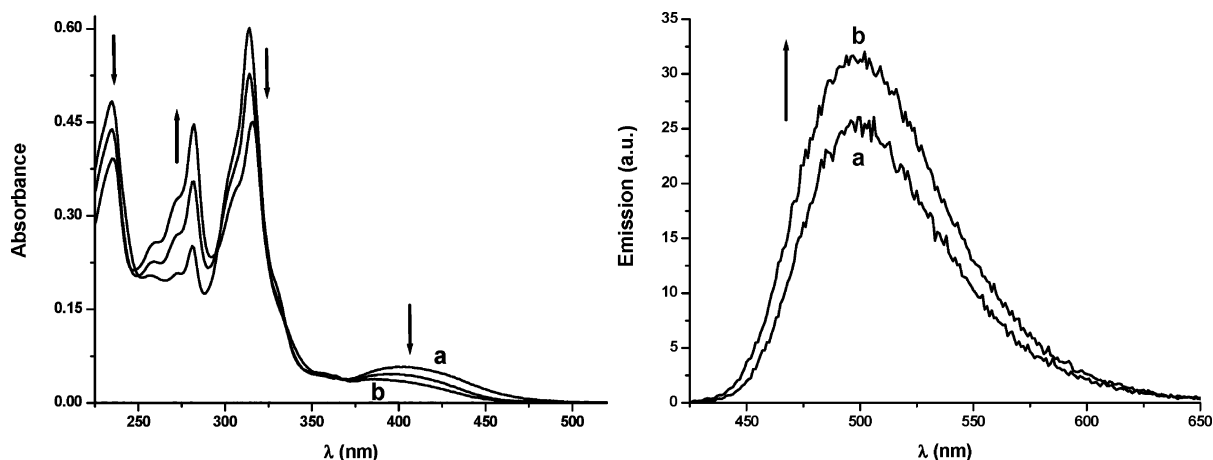
Figure 3. Changes in the absorption (left) and emission (right) spectra of compound **BIM** upon addition of Zn(II)−cyclen in acetonitrile (a) **BIM** $(2.5 \times 10^{-5}$ mol L^{-1}) and (b) **BIM/Zn** in the presence of 1 equiv of TEA.
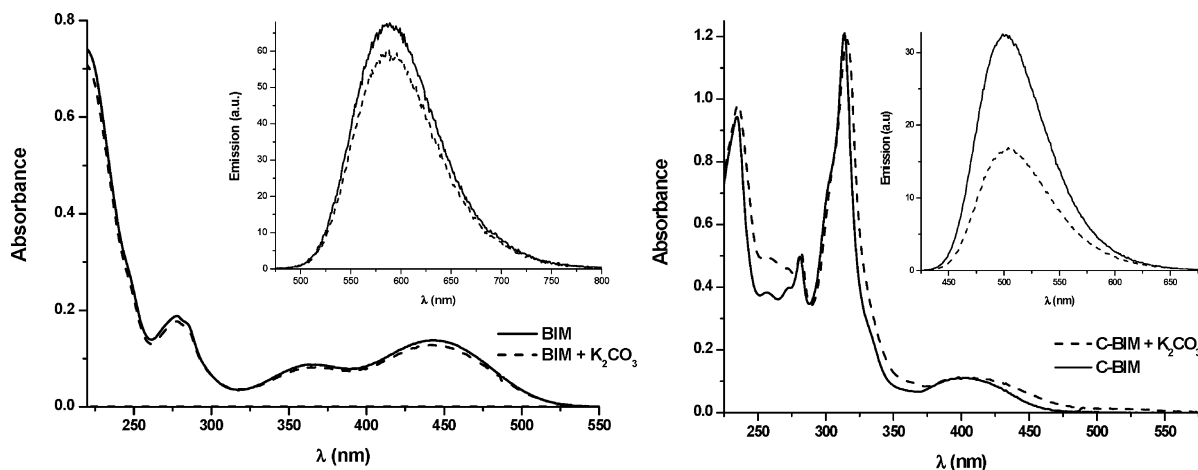

Figure 4. Changes in the absorption (left) and emission (right) spectra of compound **C-BIM** upon addition of Zn(II)−cyclen in acetonitrile (a) **C-BIM** $(2.5 \times 10^{-5}$ mol L^{-1}) and (b) **C-BIM/Zn** in the presence of 1 equiv of TEA.

Figure 5. Changes in the absorption and emission (insets) spectra ($\lambda_{ex} = 380$ nm for **BIM**, $\lambda_{ex} = 390$ nm for **C-BIM**) of **BIM** and **C-BIM** upon addition of potassium carbonate (K$_2$CO$_3$) in acetonitrile.

solutions were excited in the isosbestic point (350 nm), and the spectra are depicted in Figure 3.

Similar titration experiments were performed with compound **C-BIM** and Zn(II)−cyclen, and adduct formation was followed by UV−vis absorption and emission spectroscopy (Figure 4). In the presence of a weak base (1 equiv of TEA), the addition of Zn(II)−cyclen resulted in a blue shift (765 cm^{-1}) of the 402 nm absorption band, as was observed for **BIM**. A decrease of the molar extinction coefficients of some of the absorption bands (234, 314, and 402 nm) and an increase of the 280 nm band have been observed, which indicates complex formation (Figure

4). Binding of **C-BIM** with Zn(II)−cyclen did not influence the emission properties of **C-BIM,** as only a slight increase in emission intensity was observed (see Figure 4). The solutions were excited in the isosbestic point (335 nm).

To check whether specific interactions between the Zn(II)−cyclen and the bisindolylmaleimide systems are detrimental for the observed spectroscopic behavior and it is not just a deprotonation effect, the interaction with a strong base was studied. The absorption and emission spectra of **BIM** in the absence and presence of potassium carbonate were recorded in acetonitrile, as reported in Figure 5. For the deprotonated,

Symmetric Indolylmaleimide Derivatives

J. Phys. Chem. A, Vol. 109, No. 29, 2005 **6445**

TABLE 3: Emission Maxima and Lifetimes for BIM, C-BIM, and N-BIM in Several Solvents[a]

	BIM		C-BIM		N-BIM	
solvents	λ_{em} (nm)	τ^b (ns)	λ_{em} (nm)	τ^b (ns)	λ_{em} (nm)	τ^b (ns)
Chex	*c*	*c*	*c*	*c*	556	13.0
TOL	552	9.5	465		580	11.0
DBE	550	7.1	461	8.0	570	7.7
DIE	544	10.0	450	7.3	570	10.6
EA	560	10.7	473	8.6	585	11.3
THF	567	10.5	475	8.6	586	12.0
DCM	582	8.3	492	7.1	613	9.2
DMF	584	8.2	503	13.0	612	9.0
EtOH	640	0.4	550	7.7	646	1.4
ACN	585	8.5	499	10.0	610	9.9

[a] Data are in increasing order of polarity of solvents. See Table 1 for abbreviations. [b] Excitation wavelength is 324 nm. [c] Compounds cannot be dissolved.
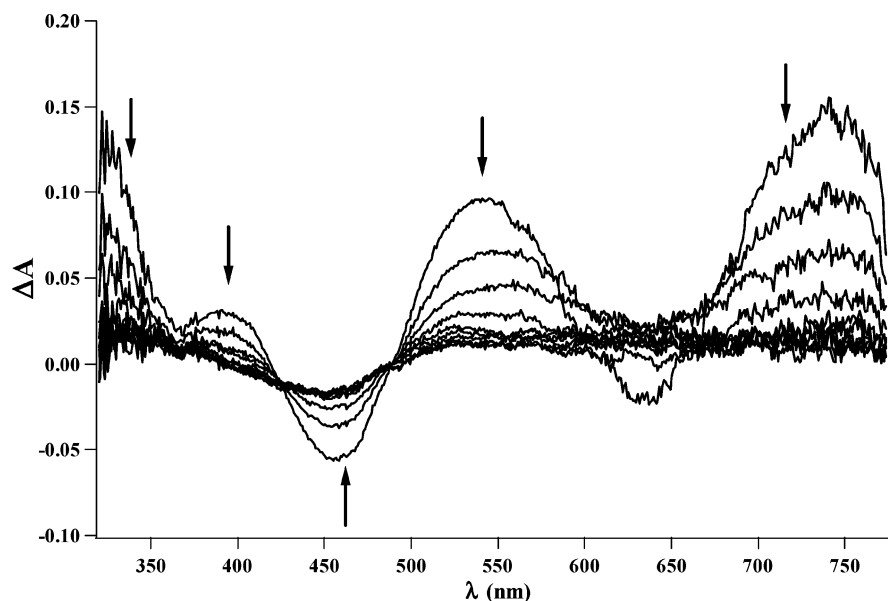

Figure 6. Transient spectra of **BIM** in deaerated acetonitrile, recorded with 5 ns increment delays (10 frames; $OD_{460} = 0.45$, $\lambda_{ex} = 460$ nm, 2 ns fwhm).

potassium-complexed **BIM,** no change in absorption and only a slight decrease in emission intensity were observed (Figure 5). For **C-BIM,** a small bathochromic shift in absorption and a significant decrease in the emission intensity upon addition of base were recorded (see Figure 5). Interestingly, these results for **C-BIM** are just the opposite of the observations for complex formation with Zn(II)−cyclen. Hence, we can conclude that the effects of coordination with Zn(II)−cyclen on the spectral characteristics cannot be explained by deprotonation alone.

Time-Resolved Spectroscopy. Whereas the asymmetric indolylmaleimide systems[11,12] show a strong increase in emission intensity upon complexation with Zn−cyclen, the symmetric systems **BIM** and **C-BIM** do not show this behavior. This already suggests that the nature of the excited state of both classes of compounds is different. To understand the role and nature of the excited states, time-resolved spectroscopy was employed.

Time-Resolved Emission Spectroscopy. Time-resolved emission spectroscopy in several solvents of different polarity and with different hydrogen-bonding properties was performed on **BIM, N-BIM**, and **C-BIM**. The emission lifetimes are summarized in Table 3. The excited-state lifetimes of all compounds show a trend similar to the emission quantum yields (see Table 1). In the cases of **BIM** and **N-BIM**, the shortest lifetimes are observed in ethanol, and in this solvent also the quantum yields are the lowest. It is interesting to notice that all other lifetimes

are between 7 and 13 ns, i.e., much longer than the lifetimes of the asymmetric systems.

Nano- and Femtosecond Transient Absorption Spectroscopy. Nano- and femtosecond transient absorption measurements were performed on acetonitrile solutions of **BIM**, **C-BIM**, and **N-BIM**. Transient absorption spectra in the nanosecond time scale are shown in Figures 6 and 7. As observed in the steady-state and time-resolved spectroscopic data, there is some change in the properties of these compounds when going from nonpolar to polar solvents. The question to answer is therefore whether another state, such as a charge-transfer state, as observed for the asymmetric derivatives,[11,12] can be formed upon light excitation in polar solvents.

The transient absorption spectra of **BIM** are characterized by absorption bands at 540 and 740 nm, and a corresponding ground-state bleaching is observed at 455 nm (see Figure 6). All the kinetic profiles probed at 455, 540, and 740 nm gave the same decay value ($\tau = 9$ ns). As reported in the previous sections, this corresponds to the lifetime obtained with time-resolved emission spectroscopy. Clearly the transient absorption spectra are due to the same (strongly emissive) excited state, and thus the transient spectra are attributed to the S_1-S_n absorption. No evidence for charge-separated species or other processes occurring after excitation are obtained.

In the case of **N-BIM**, we observed very similar transient absorption spectra, with positive bands at 415, 570, and 750
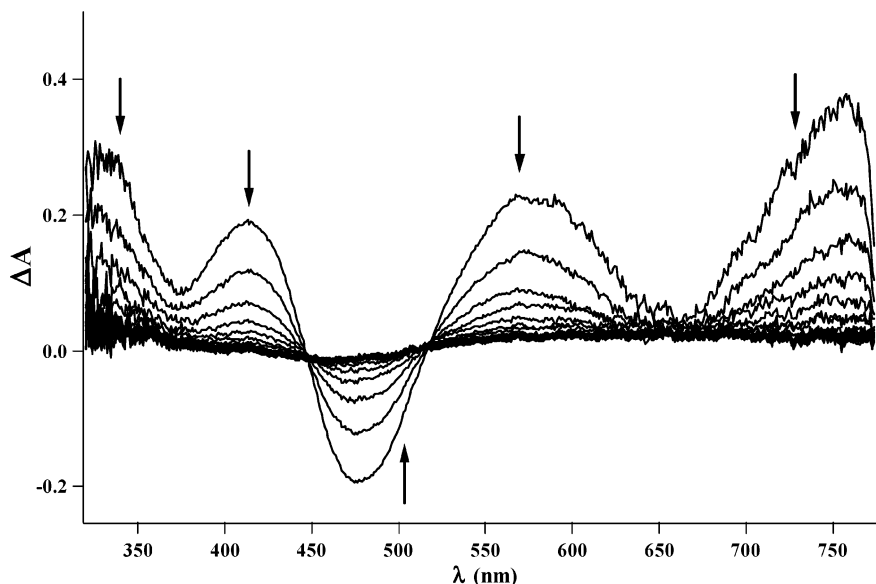
Figure 7. Transient spectra of **N-BIM** in deaerated acetonitrile, recorded with 5 ns increment delays (20 frames; OD$_{475}$ = 1.0, λ_{ex} = 475 nm, 2 ns fwhm).
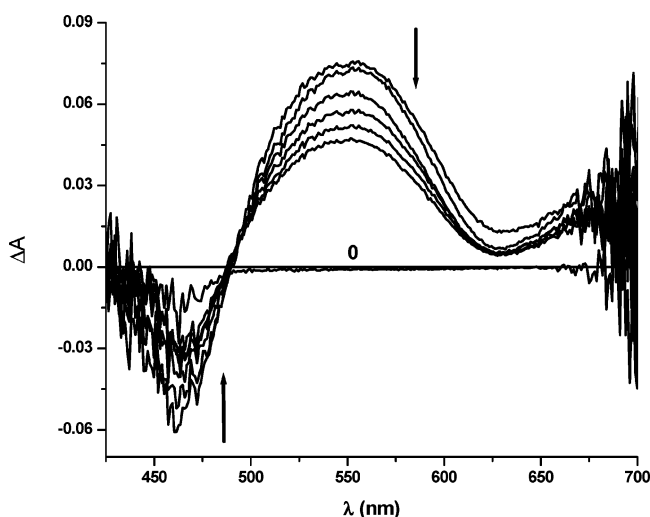

Figure 8. Femtosecond transient absorption spectra of **BIM** in aerated acetonitrile solution. Increments are 0, 2, 10, 30, 50, 70, and 90 ps. (OD$_{415}$ = 1.0, λ_{ex}= 415 nm, 130 fs fwhm).

nm and a corresponding ground-state bleaching observed at 475 nm (Figure 7). All kinetic profiles probed at 415, 570, and 750 nm resulted in the same decay value, τ = 10 ns. This corresponds well to the value found with time-resolved emission spectroscopy. Thus, these transient absorption spectra are also assigned to S$_1$–S$_n$ absorption. All transient absorption bands observed for **BIM** and **N-BIM** are formed by direct excitation and decayed with the same lifetime as the ground-state recovery. No good transient absorption spectra of **C-BIM** were obtained.

To investigate faster processes which may occur in these systems, we have performed femtosecond transient absorption spectroscopy. The spectra of **BIM** in acetonitrile were recorded between 400 and 700 nm, using excitation at 415 nm, and are depicted in Figure 8. The major characteristics of these spectra are the ground-state bleaching centered at 455 nm, the broad transient band between 480 and 625 nm, and the start of another band from 625 to 700 nm. The last spectrum recorded at 90 ps has the same profile as the transient absorption spectra recorded in the nanosecond time domain (see Figure 6). It has to be noticed that no spectral changes in time are observed. No short-lived state is observed, apart from the emissive π–π* state. So

we can conclude that upon excitation we form the emitting excited state, which is a singlet level that decays mainly radiatively to the ground state.

Computational Analysis. To support and clarify the experimental results, calculations on the molecules **BIM** and **C-BIM** were performed. The molecules were optimized with density functional theory (DFT) at the B3LYP/6-31G* level theory, using the package Gaussian-98. The optimized structures are shown in Figure 9. In the optimization the molecules were treated as isolated, and the minima found here may be different in solution.

C-BIM is a planar and symmetric molecule. The substitution of the central C–C bond connecting the two indole fragments by two hydrogen atoms leads to the more flexible and less symmetric molecule, **BIM**, where the dihedral angles of the two indole units with respect to the maleimide unit are close to 32°.

The excited states were calculated with time-dependent (TD)-DFT B3LYP/6-31G*. For each excited state, the simulation gives the oscillator strength f of the S$_0$→S$_n$ transitions. The UV–vis stick spectrum obtained was broadened with a Gaussian function (broadening constant of 2000 cm^{-1}; data are not shown) to compare with the experiments. All the main features of the experimental spectra are reproduced although deviations from experiments in the position and intensity of the absorption bands for **BIM** are larger than for the asymmetric compounds[12] and also larger than for **C-BIM** (see Table 4). The results are shown in Table 4 and compared with the experimental absorption values of **BIM** and **C-BIM** (see Figure 1). The ground-state dipole moments for **BIM** and **C-BIM** are also calculated and give a value of 6.17 and 6.22 D, respectively.

In Table 5, the energies and the composition of the first two excited states belonging to **BIM** and **C-BIM** are reported.

The representations of the main molecular orbitals (MO) involved in the excitations are depicted in Figure 10. Whereas a simple consideration on π-electron conjugation would place the first absorption band of **C-BIM** at lower energies than that of **BIM**, this is not observed. The increase of conjugation normally results in a decrease of both the HOMO–LUMO gap and the energy of S$_1$. In a series of increasingly conjugated planar molecules, for instance, this is generally true. In our case, **BIM** has a lower degree of symmetry with respect to **C-BIM**:
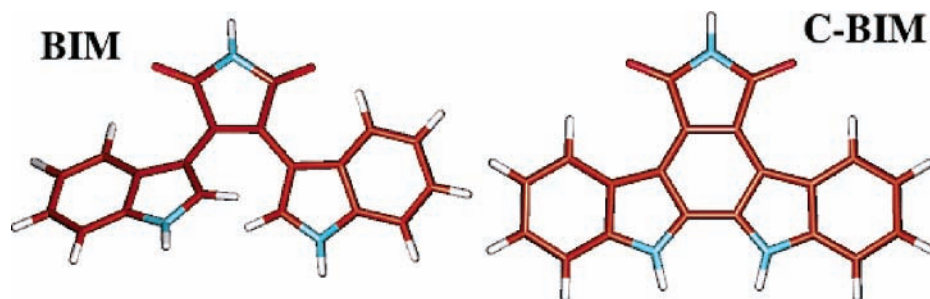
Symmetric Indolylmaleimide Derivatives

J. Phys. Chem. A, Vol. 109, No. 29, 2005 **6447**
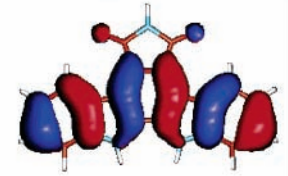
Figure 9. Optimized structures of **BIM** and **C-BIM**.
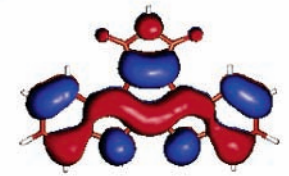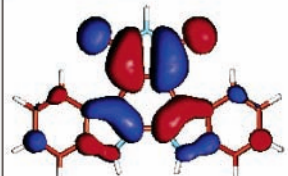
Figure 10. HOMO-1, HOMO, and LUMO of **BIM** and **C-BIM**. MO energies are written below the orbital representations. HOMO−LUMO gaps in electronvolts are **BIM** = 2.704 and **C-BIM** = 3.580.

TABLE 4: Comparison of Main Peak Positions between Experiments (Exp) and DFT Plus Broadening Simulations (Calc) (Differences (ΔE) in cm^{-1}; Ground-State Dipole Moments (μ) in Debye)

	exp^a (nm)	calc (nm)	ΔE (cm^{-1})	μ (D)
BIM	362	400	2642	6.1689
	447	570	4828	
C-BIM	398	400	126	6.2282
	314^b	296	−1937	

^{a} Recorded in toluene. ^{b} Recorded in acetonitrile.

TABLE 5: Calculated Energies (eV) and Oscillator Strengths (f) of the First Two Excited States of BIM and C-BIM (For Each State, the Composition of the Wavefunction (WF) in Terms of MO Excitations Indicated, Together with Their Coefficients in the WF Expansion)

	S$_1$	$f_{S1}{}^a$	S$_2$	$f_{S2}{}^a$
BIM	2.176 eV	0.1255	3.0268 eV	0.0399
	HOMO → LUMO		HOMO-1 → LUMO	
	(0.84)		(0.90)	
C-BIM	3.021 eV	0.0571	3.262 eV	0.0345
	HOMO → LUMO		HOMO-2 → LUMO	
	(0.15)		(0.83)	
			HOMO-1 → LUMO	
			(0.12)	

^{a} f are roughly proportional to molar extinction coefficients ϵ.

this disrupts some of the extended conjugated paths present in the more symmetric **C-BIM** (compare for example HOMOs of **BIM** and **C-BIM**) but in the meantime obeys to less limiting selections rules for the mixing of the orbitals. The result of the two effects changes the shape and ordering of MOs, which in turn affects the HOMO−LUMO gap and the energy of S$_1$. The direction of the change may be toward higher or lower energies.

The unexpected ordering of the absorbing states in **BIM** is attributed to the change of symmetry (see the following discussion and Figure 10).

From the results discussed in this section we can infer the following:

(i) The lower absorbing state is S$_1$ in both cases.

(ii) The largest MO excitation of S$_1$ is the HOMO→LUMO.

(iii) The HOMO−LUMO gap is significantly smaller for **BIM** (0.88 eV difference).

(iv) The two HOMO orbitals look very different in shape. The all-conjugated HOMO in **C-BIM** has in fact a better correspondence with the HOMO-1 in **BIM**.

The symmetry lowering in **BIM** as compared to **C-BIM** induces important orbital changes, lowering the energy of the all-conjugated HOMO in **C-BIM**−which now becomes the HOMO-1 of **BIM**−and inserting a new orbital at higher energy as the HOMO. The fact that the HOMO−LUMO gap in **C-BIM** (3.580 eV) is very close to the (HOMO-1)−LUMO gap in **BIM** (3.571 eV) supports this idea.

As pointed out earlier, the molecules already possess a high ground-state dipole moment; hence, a dramatic change upon excitation is not expected. The charge-transfer character of **BIM** and **C-BIM** has been found to be negligible. Experimentally this has been evidenced by a slight solvatochromic effect and small changes upon Zn(II)−cyclen complexation. This small charge-transfer character is endorsed by inspection of the calculated MO shapes shown in Figure 10.

If we compare the HOMO-1 of **C-BIM** to its LUMO, we clearly see that there is a reduction of electron density on the indole parts and an increase of electron density on the maleimide part.

6448 *J. Phys. Chem. A, Vol. 109, No. 29, 2005*

Kaletaş et al.

The differences between the experimental and computational values of **BIM** are larger than for **C-BIM**. This larger difference between experimental and computational values is attributed to the larger conformational freedom of **BIM**. The perturbation of the solvent can be more effective on flexible systems, with more degrees of freedom, especially if solvent-dependent conformations are present. For this reason, deviations of the calculations from the experiments are more likely to occur for **BIM**.

Conclusions

In this paper we report the photophysical properties of two natural products, arcyriarubin A (**BIM**) and arcyriaflavin A (**C-BIM**). These are symmetric indolylmaleimide derivatives containing two electron-donating indole units and an electron acceptor maleimide group. UV−vis absorption and steady-state emission measurements were performed to determine their ground- and excited-state properties in several solvents. The solvatochromic behavior of the compounds was investigated using the Kamlet−Taft solvatochromic parameters. Also the formation of assemblies with Zn(II)−cyclen was investigated using steady-state spectroscopy. Their behavior toward coordination to Zn(II)−cyclen was observed to be different from the behavior observed for the asymmetric compounds,[11,12] as both symmetric compounds did not show a significant change in the emission behavior.

To clarify the nature of the lowest excited state, time-resolved emission and nano- and femtosecond transient absorption measurements were performed in acetonitrile. The results showed that despite the strong polar character of the molecule the emissive state is a $\pi-\pi^*$ excited state and that the large conjugation is responsible for the color and emission properties of the compounds. These conclusions were supported by the computational studies which show that the molecular orbitals in **BIM** and **C-BIM** are delocalized over the whole molecule. There are no occupied or unoccupied orbitals that have coefficients only on the indole part or on the maleimide moiety. Thus, the calculations do not indicate any transition with a strong charge-transfer character.

Experimental Section

Materials. All solvents used are spectroscopic grade and purchased from Acros and Merck Uvasol and used as received unless otherwise indicated. Commercially available deuterated solvents were used as received for the characterization of the compounds. NMR spectra were recorded on a Bruker AC-200 and Bruker AC-300 MHz instrument at ambient temperature. Data were recorded as follows: chemical shift in ppm from internal standard TMS on the δ scale, multiplicity (s = singlet, d = doublet, t = triplet), and assignment. For column chromatography, Merck silica gel 60 was used. Thin-layer chromatography (TLC) was performed on TLC aluminum sheet silica gel 60 F_{254}. Electron impact (EI) and fast atom bombardment (FAB+) mass spectra were carried out using a JEOL JMS SX/SX102A four-sector mass spectrometer. The samples were introduced via the direct insertion probe into the ion source.

All reagents used were obtained from available commercial sources and used without additional purification unless otherwise indicated. The synthesis of 2,3-bis(1*H*-indol-3-yl)maleimide (**BIM**) was done according to a known procedure from the literature.[14] For the synthesis of 12,13-dihydro-5*H*-indolo[2,3-*a*]pyrrolo[3,4-*c*]carbazole-5,7-(6*H*)-diones (**C-BIM**) photochemical oxidation in acetonitrile with I_2 was applied.

Synthesis. *2,3-Bis(1H-indol-3-yl)maleimide (BIM).* To a solution of indole-3-acetamide (**1**; 1.44 mmol, 0.25 g) in 8 mL of dry THF, methyl indolyl-3-glyoxylate (**2**; 1.58 mmol, 0.32 g) was added under nitrogen atmosphere. The mixture was cooled to 0 °C. To this solution, potassium *tert*-butoxide (4.3 mmol, 4.3 mL of a 1.0 M solution in THF) was added dropwise. The mixture was allowed to warm to room temperature (RT) and further was stirred for 3 h. To quench the reaction, 3 mL of concentrated HCl (37%) was added. The solution was diluted with 50 mL of ethyl acetate. The organic layers were washed with water (2 × 50 mL) and 20 mL of brine. The organic phase was collected and dried with MgSO₄. The solvent was evaporated under vacuum, and the crude product (dark red oil) was purified by column chromatography (SiO₂; hexane/ethyl acetate of (1) 2:1 and (2) 1:1). The yield of the product was 93%. See also ref 12. ¹H NMR (200 MHz, DMSO-d_6): δ 11.7 (s, 2H, NH), 10.95 (s, 1H, imide-NH), 7.75 (d, 2H, aromatic H), 7.38 (d, 2H, J = 7.7 Hz, aromatic H), 7.00 (t, 2H, J = 7.7 Hz, aromatic H), 6.84 (d, 2H, J = 7.7 Hz, aromatic H), 6.65 (t, 2H, J = 7.7 Hz, aromatic H). ¹³C NMR (50 MHz, DMSO-d_6): δ 173.0, 136.0, 129.04, 127.7, 125.4, 121.5, 120.9, 119.5, 111.7, 105.6. MS (FAB+): m/z (%)328.1.

12,13-Dihydro-5H-indolo[2,3-a]pyrrolo[3,4-c]carbazole-5,7-(6H)-diones (C-BIM). A mixture of 2,3-bis(1*H*-indol-3-yl)-maleimide (**BIM**; 0.104 g, 0.32 mmol) and I₂ (12 mg, 0.046 mmol) was dissolved in 20 mL of acetonitrile and stirred. The solution was placed in a quartz container and irradiated with a Rayonet preparative photochemical reactor at 350 nm for overnight. The reaction was cooled to room temperature; the precipitate was collected by filtration and recrystallized from acetone to yield 87% (0.090 g) of an orange solid. ¹H NMR (300 MHz, DMSO-d_6): δ 11.74 (s, 2H), 10.98 (s, 1H), 8.99−8.97 (d, 2H), 7.82−7.80 (d, 2H), 7.57 (m, 2H), 7.36 (m, 2H). MS (EI): m/z (%)325.1 (100, M⁺·).

Instrument Methods. *Steady-State Spectroscopy.* Electronic absorption spectra were recorded on a Hewlett-Packard UV−vis, diode array 8453 spectrophotometer.

Steady-state emission spectra were obtained from SPEX 1681 Fluorolog spectrofluorometer equipped with two double monochromators (excitation and emission). Emissions are not corrected. Quantum yields of the compounds were calculated relative to quinine bisulfate solution in 1 N H₂SO₄ solution as reference, in all solvents.[25]

Time-Resolved Spectroscopy. Time-resolved fluorescence emission measurements were performed on a picosecond single photon counting (SPC) setup. The frequency-doubled (300−340 nm, 1 ps, 3.8 MHz) output of a cavity-dumped DCM dye laser (Coherent model 700) pumped by a mode-locked Ar-ion laser (Coherent 486 AS Mode Locker, Coherent Innova 200 laser) was used as the excitation source. A (Hamamatsu R3809) microchannel plate photomultiplier was used as detector. The instrument response (~17 ps full width at half-maximum (fwhm)) was recorded using the Raman scattering of a doubly deionized water sample. Time windows (4000 channels) of 5 ns (1.25 ps/channel) to 50 ns (12.5 ps/channel) could be used, enabling the measurement of decay times of 5 ps to 40 ns. The recorded traces were deconvoluted with the system response and fitted to an exponential function using the Fluofit (Pico-Quant) windows program.

In nanosecond pump−probe experiments, for excitation a (Coherent) Infinity Nd:YAG−XPO laser was used. The laser illuminated a slit of 10 × 2 mm. Perpendicular to this, the probe light provided by an EG&G (FX504) low-pressure xenon lamp irradiated the sample through a 1 mm pinhole. The overlap of

Symmetric Indolylmaleimide Derivatives

J. Phys. Chem. A, Vol. 109, No. 29, 2005 **6449**

the two beams falls within the first 2 mm of the cell, after the slit. The probe light from both the signal and the reference channels is then collected in optical fibers which are connected to an Acton SpectraPro-150 spectrograph which is coupled to a Princeton Instruments ICCD-576-G/RB-EM gated intensified CCD camera. Using a 5 ns gate, this camera simultaneously records the spectrally dispersed light from both optical fibers on separate stripes of the CCD.

In femtosecond transient absorption measurements, Spectra-Physics Hurricane titanium:sapphire regenerative amplifier system was used as the laser system. The full-spectrum setup was based on an optical parametric amplifier (Spectra- Physics OPA 800) as a pump. A residual fundamental light, from the pump OPA, was used for white light generation, which was detected with a CCD spectrograph. The OPA was used to generate excitation pulses at 345 and 575 nm. The laser output was typically 5 μJ pulse^{-1} (130 fs fwhm) with a repetition rate of 1 kHz. A circular cuvette ($d = 1.8$ cm, 1 mm; Hellma), with the sample solution, was placed in a homemade rotating ball bearing (1000 rpm), to avoid local heating by the laser beam. The solutions of the samples were prepared to have an optical density at the excitation wavelength of ca. 0.5 in a 1 mm cell. The absorbance spectra of the solutions were measured before and after the experiments, to check for degradation.

References and Notes

(1) Nishizuka, Y. *Nature* **1984**, *308*, 693−698.

(2) Bit, R. A.; Davis, P. D.; Elliott, L. H.; Harris, W.; Hill, C. H.; Keech, E.; Kumar, H.; Lawton, G.; Maw, A.; Nixon, J. S.; Vesey, D. R.; Wadsworth, J.; Wilkinson, S. E. *J. Med. Chem.* **1993**, *36*, 21−29.

(3) Davis, P. D.; Hill, C. H.; Lawton, G.; Nixon, J. S.; Wilkinson, S. E.; Hurst, S. A.; Keech, E.; Turner, S. E. *J. Med. Chem.* **1992**, *35*, 177−184.

(4) Tamaoki, T.; Nomoto, H.; Takahashi, I.; Kato, Y.; Morimoto, M.; Tomita, F. *Biochem. Biophys. Res. Commun.* **1986**, *38*, 397−402.

(5) Steglich, W.; Steffan, B.; Eckhardt, L. K. *Angew. Chem.* **1980**, *92*, 463−464.

(6) Mahboobi, S.; Eibler, E.; Koller, M.; Kumar KC, S.; Popp, A. *J. Org. Chem.* **1999**, *64*, 4697−4704.

(7) Gillig, J. R.; Jirousek, M. R. (Lilly, Eli, and Co., USA) PCT Int. Appl. WO 9535294, 1995.

(8) Mahboobi, S.; Dechant, I.; Reindl, H.; Pongratz, H.; Popp, A.; Schollmeyer, D. *J. Heterocycl. Chem.* **2000**, *37*, 307−329.

(9) Saulnier, M. G.; Frennesson, D. B.; Deshpande, M. S.; Vyas, D. M. *Tetrahedron Lett.* **1995**, *36*, 7841−7844.

(10) Chiu, C.-W.; Chow, T. J.; Chuen, C.-H.; Lin, H.-M.; Tao, Y.-T. *Chem. Mater.* **2003**, *15*, 4527−4532.

(11) Kaletas, B. K.; Williams, R. M.; König, B.; De Cola, L. *Chem. Commun.* **2002**, *7*, 776−777.

(12) Kaletas, B. K.; Joshi, H. C.; van der Zwan, G.; Fanti, M.; Zerbetto, F.; Goubitz, K.; De Cola, L.; König, B.; Williams, R. M. Manuscript in preparation.

(13) Brenner, M.; Rexhausen, H.; Steffan, B.; Steglich, W. *Tetrahedron* **1988**, *44*, 2887−2892.

(14) Faul, M.; Winneroski, L.; Krumrich, C. *J. Org. Chem.* **1998**, *63*, 6053−6058.

(15) (a) Turro, N. J. *Modern Molecular Photochemistry*; University Science Books: Herndon, VA, 1991; Chapter 6, p 184. (b) Abboud, J.-L. M.; Kamlet, M. J.; Taft, R. W. *Prog. Phys. Org. Chem.* **1981**, *13*, 485−630.

(16) Kamlet, M. J.; Abboud, J.-L. M.; Taft, R. W. *J. Am. Chem. Soc.* **1977**, *99*, 6027−6038.

(17) Kamlet, M. J.; Abboud, J.-L. M.; Taft, R. W. *J. Am. Chem. Soc.* **1977**, *99*, 8325−8327.

(18) Reichardt, C. *Chem. Rev.* **1994**, *94*, 2319−2358.

(19) Kamlet, M. J.; Abboud, J.-L. M.; Abraham, M. H.; Taft, R. W. *J. Org. Chem.* **1983**, *48*, 2877−2887.

(20) Taft, R. W.; Abboud, J.-L. M.; Kamlet, M. J. *J. Org. Chem.* **1984**, *49*, 2001−2005.

(21) Koenig, B.; Pelka, M.; Zieg, H.; Ritter, T.; Bouas-Laurent, H.; Bonneau, R.; Desvergne, J.-P. *J. Am. Chem. Soc.* **1999**, *121*, 1681−1687.

(22) Aoki, S.; Sugimura, C.; Kimura, E. *J. Am. Chem. Soc.* **1998**, *120*, 10094−10102.

(23) Kimura, E.; Kitamura, H.; Ohtani, K.; Koike, T. *J. Am. Chem. Soc.* **2000**, *122*, 4668−4677.

(24) Koike, T.; Gotoh, T.; Aoki, S.; Kimura, E.; Shiro, M. *Inorg. Chim. Acta* **1998**, *270*, 424−432.

(25) Meech, S. R.; Phillips, D. *J. Photochem.* **1983**, *23*, 193.